



Regular Article

Specific interactions between alkali metal cations and the KcsA channel studied using ATR-FTIR spectroscopy

Yuji Furutani^{1,2}, Hirofumi Shimizu³, Yusuke Asai², Shigetoshi Oiki³ and Hideki Kandori²

¹Department of Life and Coordination-Complex Molecular Science, Institute for Molecular Science, Okazaki, Aichi 444-8585, Japan

²Department of Frontier Materials, Nagoya Institute of Technology, Nagoya, Aichi 466-8555, Japan

³Department of Molecular Physiology and Biophysics, Faculty of Medical Sciences, University of Fukui, Matsuoka, Fukui 910-1193, Japan

Received July 7, 2015; accepted August 21, 2015

The X-ray structure of KcsA, a eubacterial potassium channel, displays a selectivity filter composed of four parallel peptide strands. The backbone carbonyl oxygen atoms of these strands solvate multiple K⁺ ions. KcsA structures show different distributions of ions within the selectivity filter in solutions containing different cations. To assess the interactions of cations with the selectivity filter, we used attenuated total reflection Fourier-transform infrared (ATR-FTIR) spectroscopy. Ion-exchange-induced ATR-FTIR difference spectra were obtained by subtracting the spectrum of KcsA soaked in K⁺ solution from that obtained in Li⁺, Na⁺, Rb⁺, and Cs⁺ solutions. Large spectral changes in the amide-I and -II regions were observed upon replacing K⁺ with smaller-sized cations Li⁺ and Na⁺ but not with larger-sized cations Rb⁺ and Cs⁺. These results strongly suggest that the selectivity filter carbonyls coordinating Rb⁺ or Cs⁺ adopt a conformation similar to those coordinating K⁺ (cage configuration), but those coordinating Li⁺ or Na⁺ adopt a conformation (plane configuration) considerably different from those coordinating K⁺. We have identified a cation-type sensitive amide-I band at 1681 cm⁻¹ and an insensitive amide-I band at 1659 cm⁻¹. The bands at 1650, 1639, and 1627 cm⁻¹ observed for Na⁺-coordinating carbonyls were almost identical to those observed in Li⁺ solution, suggesting

that KcsA forms a similar filter structure in Li⁺ and Na⁺ solutions. Thus, we conclude that the filter structure adopts a collapsed conformation in Li⁺ solution that is similar to that in Na⁺ solution but is in clear contrast to the X-ray crystal structure of KcsA with Li⁺.

Key words: Vibrational spectroscopy, Ion-protein interaction, Ion selectivity, Coordination chemistry

KcsA is a potassium channel from the eubacterium *Streptomyces lividans* [1]. The X-ray structure of the KcsA channel was the first channel protein structure solved [2]. Extensive experimental and theoretical studies have led the KcsA channel to be used as a model channel for the study of the structure–function relationships of selective ion permeation [3–8]. The tetrameric structure has a four-fold axis; the pore exists along this axis (Fig. 1a). Each monomer is composed of two transmembrane helices, an outer helix called TM1 and an inner tilted helix called TM2 as well as a short helix called the pore helix. The signature sequence TVGYG is responsible for the selective permeability of potassium channels.

The X-ray structure of KcsA revealed a specific role of the peptide backbone of the signature sequence in ion selectivity. Rather than forming secondary structures, the backbone of the signature sequence is linearly extended, and the four strands from subunits align in parallel to form a narrow pore. The backbone C=O groups from the four strands orient their oxygen atoms centripetally towards K⁺ ions aligned on the symmetry axis. In this configuration, the carbonyl oxygens solvate dehydrated K⁺ ions. There are at least four binding sites in the selectivity filter. Intimate interactions between

Corresponding authors: Yuji Furutani, Department of Life and Coordination-Complex Molecular Science, Institute for Molecular Science, 38 Nishigo-Naka, Myodaiji, Okazaki, Aichi 444-8585, Japan. e-mail: furutani@ims.ac.jp; Hideki Kandori, Department of Frontier Materials, Nagoya Institute of Technology, Showa-ku, Nagoya, Aichi 466-8555, Japan. e-mail: kandori@nitech.ac.jp; Shigetoshi Oiki, Department of Molecular Physiology and Biophysics, Faculty of Medical Sciences, University of Fukui, Matsuoka, Fukui 910-1193, Japan. e-mail: oiki-fki@umin.ac.jp

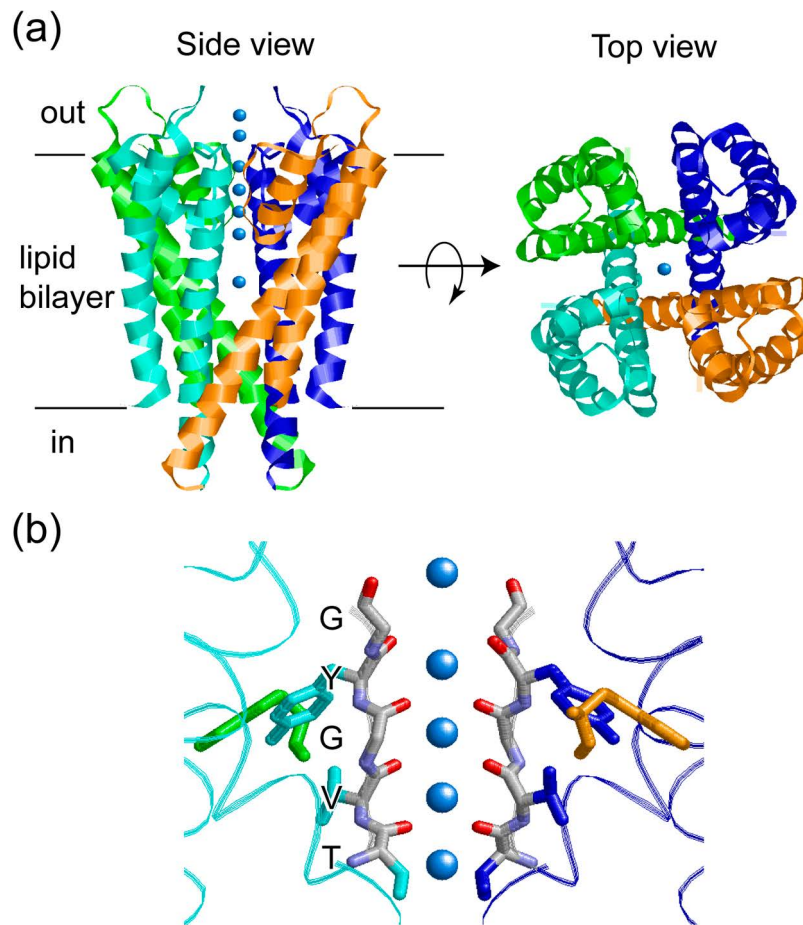


Figure 1 (a) X-ray structure of KcsA. KcsA forms a homo-tetramer that includes a pore in the center of the monomers, which are shown in different colors. Each monomer has two transmembrane helices and a short helix connected by a TVGYG sequence that is highly conserved in potassium ion channels. Potassium ions are colored sky blue. (b) Structure of the ion selectivity filter. The carbonyl groups of the main chains of the TVGYG sequences constitute the selectivity filter (stick drawing). The side chains of Trp68 and Tyr78, which are shown using stick drawings, are located within hydrogen-bonding distance.

the selectivity filter and K^+ ions maintain the filter structure even without the formation of hydrogen bonds within the filter backbone. Furthermore, in the back of the pore lining, the side chains of the TVGYG interact with the residues of the pore helix to stabilize the selectivity filter structure. Figure 1b shows that Tyr78 in the signature sequence and Trp68 on the pore helix interact with each other by forming a hydrogen bond which is effective for stabilization of the tetrameric structure of KcsA [9]. These structural features allow the peptide backbone to be directly involved in the specific recognition and permeation of K^+ ions.

X-ray crystallographic studies of KcsA with several alkali metal cations (Fig. 2) have shown that the selectivity filters in the K^+ -, Rb^+ -, Cs^+ -, and Li^+ -bound species adopt very similar structures [10–13]. On the other hand, the Na^+ -bound conformation differs substantially; the peptide backbone near Gly77 is flipped into the inside of the pore, forming the so-called “collapsed” conformation [12]. The positions of alkali metal cations along the pore axis are somewhat differ-

ent than that of K^+ ions. A K^+ ion is coordinated by eight carbonyl groups in each binding site (cage configuration). In contrast, a Na^+ ion is coordinated by four carbonyl groups (plane configuration). Even though the crystal structure of the KcsA channel in Li^+ solution adopts the conductive conformation of the selectivity filter, a Li^+ ion is assumed to be coordinated by four carbonyl groups (The proposed position of Li^+ ion is indicated by a filled-in blue circle in Fig. 2.) [13]. Further analysis of the structures of the selectivity filter with these alkali metal cations is needed to understand the ion selectivity of KcsA.

Stimulus-induced difference Fourier-transform infrared (FTIR) spectroscopy is a powerful tool for investigating the protein structural changes that accompany biologically important functional processes. This method has been extensively applied to photoactive proteins [14–17] and has been shown to allow detailed structural analysis, including changes in hydrogen-bonding of even a single water molecule [18–21]. However, it has not been easy to apply this technique to

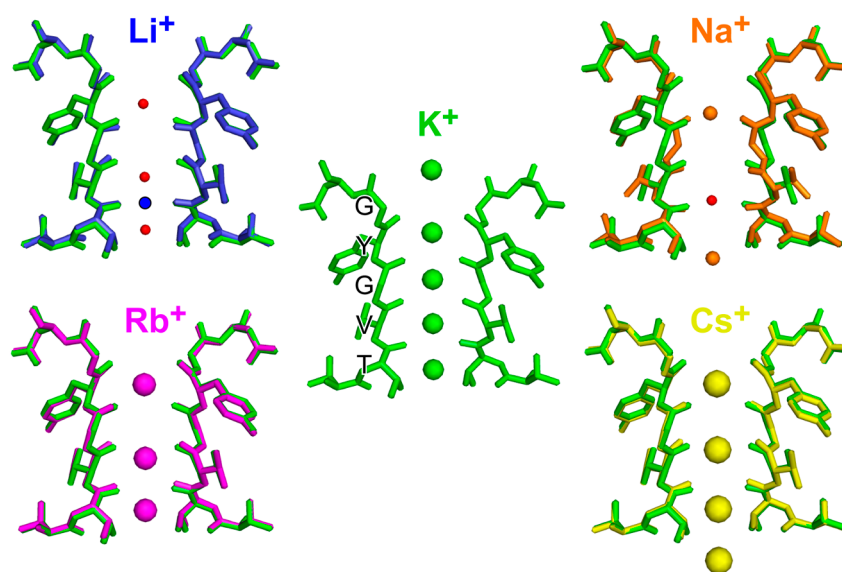


Figure 2 Structures of the ion selectivity filter in KcsA(Li⁺) [13], KcsA(Na⁺) [12], KcsA(K⁺) [10], KcsA(Rb⁺) [11], and KcsA(Cs⁺) [11], where the KcsA(K⁺) structure (green) is superimposed on each structure. Red circles represent oxygen atoms of water molecules.

other stimuli, such as voltage and ligand binding. Attenuated Total Reflection (ATR)-FTIR spectroscopy uses samples that are bathed in aqueous solution, so that solution pH and ionic composition can be preserved and accurately controlled [22,23]. Consequently, redox-induced and ligand binding-induced ATR-FTIR difference spectra have provided detailed mechanisms, at atomic resolution, for the reactions of several membrane proteins, including respiratory cytochrome bc₁ complex [24], cytochrome *c* oxidase [25–27], Na⁺/galactose transporter [28], transhydrogenase [29], melibiose permease [30], microbial rhodopsins [31–33], flagellar motor PomA–PomB complex [34], and V-type Na⁺-ATPase [35], to these stimuli. In 2012, we applied the ATR-FTIR technique to the study of KcsA and tentatively assigned the amide I modes of the selectivity filter, which change their frequencies upon replacement of K⁺ with Na⁺ in buffer solution at neutral pH [36]. The apparent K_D for K⁺ binding obtained from these spectra was ~9 mM [36]. Surface-enhanced infrared absorption spectroscopy (SEIRA), which has further enabled voltage-induced difference spectroscopy of membrane proteins in monolayers [37], was recently applied to KcsA as well [38,39]. Thus, the ATR-FTIR technique is a promising method for the study of structure–function relationships in membrane proteins.

In this study, to better understand the ion-selectivity of the channel, we extended the ATR-FTIR spectroscopic studies of KcsA by replacing K⁺ or Na⁺ with various alkali metal cations. Repeated measurements provided highly accurate difference FTIR spectra between the two of monovalent cations (Li⁺, Na⁺, K⁺, Rb⁺, and Cs⁺). Large spectral changes in the amide-I and -II regions were seen when comparing the spectra of complexes containing smaller cations (Li⁺, Na⁺)

with the spectra of those containing larger cations (K⁺, Rb⁺, Cs⁺). These changes reflect a difference between the local structures of the selectivity filters interacting with these cations. We discuss the structural role of the selectivity filter in KcsA on the basis of the present ATR-FTIR results.

Materials and Methods

Preparation of KcsA samples; Expression, Purification and Reconstitution into Liposomes. KcsA samples were prepared according to a previously described method [40]. The gene encoding the wild-type KcsA channel was inserted into plasmid vector pQE-82L (QIAGEN, Valencia, CA), which was used to transform *Escherichia coli* BL21 cells. Protein expression was induced by addition of 0.5 mM isopropyl-β-D-thiogalactopyranoside. *E. coli* cells expressing KcsA channels were broken up by sonication, and the membrane fractions were solubilized in buffer (20 mM potassium phosphate, pH 7.5, 200 mM KCl, 20 mM 2-mercaptoethanol, 50 mM imidazole) containing 1% *n*-dodecyl-β-D-maltoside (DDM; Dojindo, Kumamoto, Japan). Histidine-tagged channels were purified with a Co²⁺-based metal-chelate affinity chromatography resin. Purified channels, which were eluted using 100–400 mM imidazole, had protein concentrations of 0.5–3 mg/mL. The purified samples were mixed with lipids 1-palmitoyl-2-oleoyl phosphatidylethanolamine (POPE) / 1-palmitoyl-2-oleoyl phosphatidylglycerol (POPG) (w/w=3:1) at a molar ratio of 1:100. To reconstitute the purified KcsA proteins into liposomes, DDM was removed by size-exclusion gel column chromatography. Finally, the proteoliposomes were suspended in buffer (20 mM HEPES, pH 7.5, 200 mM KCl) and the protein concentration was adjusted to 1 mg/mL.

Perfusion-Induced ATR-FTIR Spectroscopy. A 5- μ L aliquot of liposomes containing KcsA (\sim 1 mg/mL) was placed on the surface of a diamond ATR crystal (Smiths Detection, DurasamplIR II; 9 effective internal reflections). After drying in a gentle stream of N_2 , the sample was rehydrated by flowing perfusion buffer (20 mM HEPES, pH 7, containing 50 mM NaCl) through the system. Before measuring ion-exchange-induced difference spectra, the sample was perfused with the same buffer at a flow rate of 0.5 mL/min for 100 min to remove excess buffer and impurities concentrated upon drying. ATR-FTIR spectra of the KcsA sample were recorded at 293 K and 2 cm^{-1} resolution using a Bio-Rad FTS-6000 spectrometer, equipped with a liquid-nitrogen-cooled mercury cadmium telluride detector [32,34]. First, a background spectrum of the film was recorded during perfusion with buffer in the presence of 50 mM NaCl for 15 min (an average of 1710 interferograms). The buffer was then switched to one containing 50 mM KCl. After a 5-min delay for equilibration, a K^+ -minus- Na^+ difference spectrum was recorded for 15 min (an average of 1710 interferograms). After a new background spectrum was taken, the buffer was switched

back to 50 mM NaCl. After 5-min delay, an equivalent Na^+ -minus- K^+ difference spectrum was recorded. This cycling procedure was repeated 8–16 times. The final difference spectra were calculated as the average of the K^+ -minus- Na^+ spectra and the average of the Na^+ -minus- K^+ spectra multiplied by -1 . Measurements for Li^+ , Rb^+ , and Cs^+ were done similarly. The buffer pH was adjusted using LiOH, NaOH, KOH, RbOH, or CsOH. The flow rate was maintained at 0.5 mL/min.

Results and Discussion

Difference FTIR Spectra of KcsA induced by Alkali Metal Cation Exchange. The K^+ -minus- Na^+ difference spectrum (see Methods) shown in Figure 3 displays the characteristic vibrations of KcsA that correspond to its interaction with K^+ (positive side) or Na^+ (negative side), as reported previously [36]. To gain further information, we compared difference FTIR spectra among alkali metal cations (Li^+ , Na^+ , K^+ , Rb^+ , and Cs^+), where we first measured the difference spectra between K^+ and the other cations, and then measured the

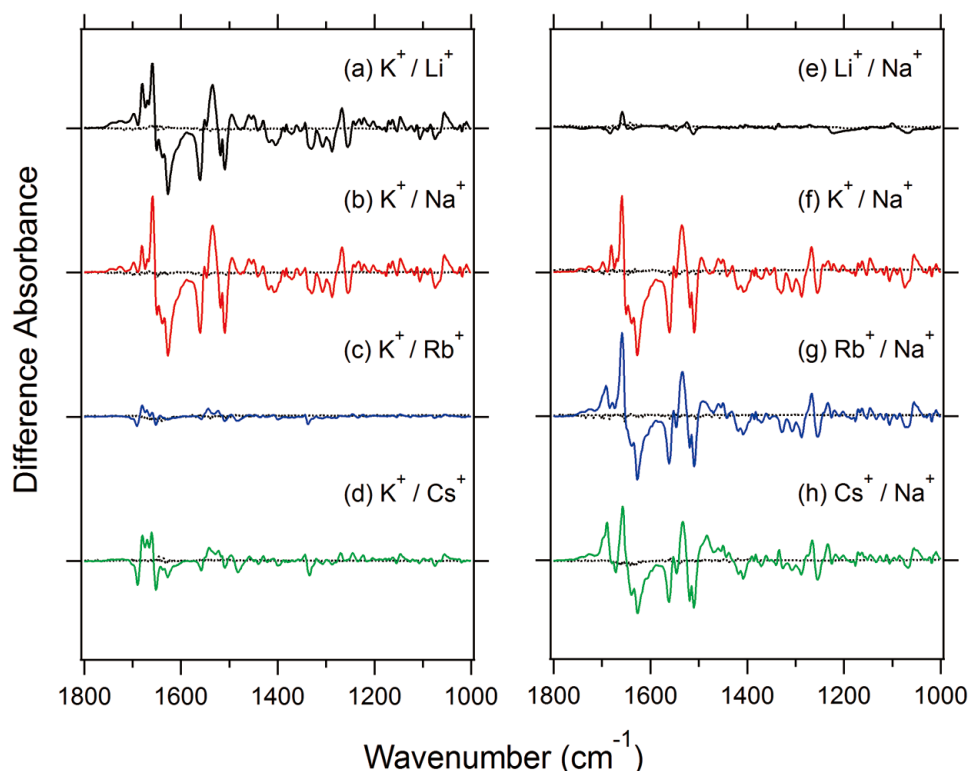


Figure 3 (Left panel) Solid curves represent the K^+ -minus- Li^+ (a), K^+ -minus- Na^+ (b), K^+ -minus- Rb^+ (c), and K^+ -minus- Cs^+ (d) FTIR difference spectra of KcsA recorded at pH 7 and 293 K. Dotted curves are the Li^+ -minus- Li^+ (a), Na^+ -minus- Na^+ (b), Rb^+ -minus- Rb^+ (c), and Cs^+ -minus- Cs^+ (d) FTIR difference spectra of KcsA. The same KcsA sample on the ATR cell was used for the measurements, so that amplitudes of these spectra can be compared. Namely, small spectral changes indicate similar protein structure between K^+ and each monovalent cation. One division of the y-axis represents 0.015 absorbance units. (Right panel) Solid curves represent the Li^+ -minus- Na^+ (e), K^+ -minus- Na^+ (f), Rb^+ -minus- Na^+ (g), and Cs^+ -minus- Na^+ (h) FTIR difference spectra of KcsA recorded at pH 7 and 293 K. Dotted curves are the Li^+ -minus- Li^+ (e), K^+ -minus- K^+ (f), Rb^+ -minus- Rb^+ (g), and Cs^+ -minus- Cs^+ (h) FTIR difference spectra of KcsA. The same KcsA sample on the ATR cell was used for the measurements, and small spectral changes indicate similar protein structure between Na^+ and each monovalent cation. One division of the y-axis represents 0.015 absorbance units.

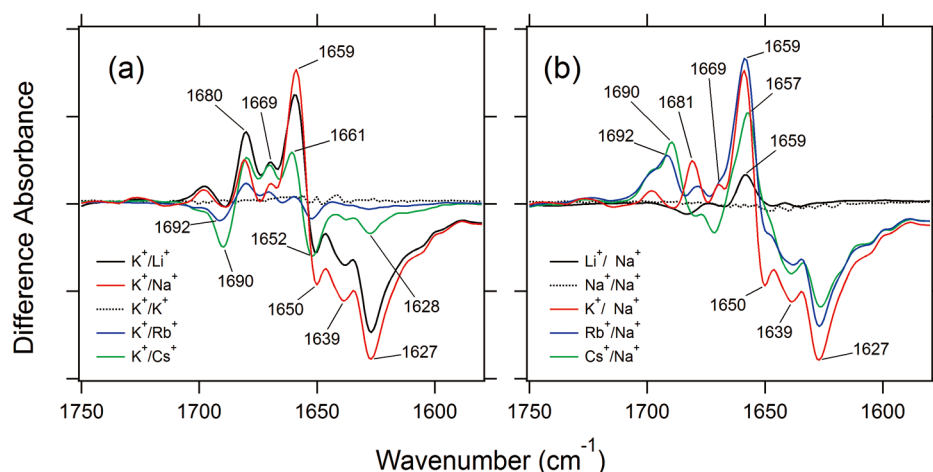


Figure 4 ATR-FTIR difference spectra of KcsA in the amide-I region (1750–1580 cm^{-1}), reproduced from Figure 2. (a) The K^+ -minus- Li^+ (black solid curve), K^+ -minus- Na^+ (red curve), K^+ -minus- K^+ (black dotted curve), K^+ -minus- Rb^+ (blue curve), and K^+ -minus- Cs^+ (green curve) spectra. (b) The Li^+ -minus- Na^+ (black solid curve), Na^+ -minus- Na^+ (black dotted curve), K^+ -minus- Na^+ (red curve), Rb^+ -minus- Na^+ (blue curve), and Cs^+ -minus- Na^+ (green curve) spectra. One division of the y-axis represents 0.005 absorbance units.

difference spectra between Na^+ and the other cations. Each spectrum was normalized to the amplitude of the amide-II peak in the absorption spectrum of a KcsA sample in the reference buffer (K^+ or Na^+). The left panel of Figure 3 compares the FTIR difference spectra of K^+ and the other cations, where spectral changes are greatest and smallest for the K^+ -minus- Na^+ and K^+ -minus- Rb^+ difference spectra, respectively. The K^+ -minus- Li^+ difference spectrum is similar to the K^+ -minus- Na^+ spectrum, though the intensity is slightly smaller. The intensity of the K^+ -minus- Cs^+ difference spectrum is between those of the K^+ -minus- Rb^+ and K^+ -minus- Li^+ spectra. Thus, the structures of KcsA in K^+ (KcsA(K^+)) and Rb^+ solutions (KcsA(Rb^+)) are similar. Similarly, the right panel of Figure 3, showing the FTIR difference spectra of Na^+ and the other cations supports the contrast among the alkali cation spectra. We analyzed the difference spectra in the amide-I and -II vibrational regions in detail, as described below.

Amide-I Vibrations of KcsA Interacting with Alkali Metal Cations. Figure 4a and 4b compare FTIR difference spectra between K^+ and the other cations and between Na^+ and the other cations, respectively, in the amide-I vibrational region. As already mentioned, KcsA(K^+), KcsA(Rb^+), and KcsA(Cs^+) exhibited similar spectral patterns and KcsA(Na^+) and KcsA(Li^+) exhibited similar spectral patterns. From this comprehensive analysis, we obtained characteristic amide-I frequencies of KcsA with each cation, which are summarized in Table 1. KcsA(K^+), KcsA(Rb^+), and KcsA(Cs^+) possess a strong peak at 1659 or 1657 cm^{-1} and a moderate peak at 1681 cm^{-1} (K^+), 1692 cm^{-1} (Rb^+), and 1690 cm^{-1} (Cs^+). On the other hand, KcsA(Na^+) and KcsA(Li^+) possess strong peaks at 1650, 1639, and 1627 cm^{-1} , among which the 1627- cm^{-1} band is the strongest. The lower frequency shift of the amide-I vibrations can be explained by a stronger hydro-

gen-bonding or ionic interaction, or a change in the transition dipole coupling of the backbone carbonyl groups [41]. In the previous study, we tentatively assigned the amide I vibrations for KcsA(K^+) and KcsA(Na^+) to the carbonyl groups forming the eight-coordinate structure with K^+ and the four-coordinate structure with Na^+ , respectively [36]. Here, the observed amide-I vibrations are classified as higher frequency for KcsA(K^+), KcsA(Rb^+) and KcsA(Cs^+), and lower frequency for KcsA(Na^+) and KcsA(Li^+). These results support the eight-carbonyl and four-carbonyl coordinated configurations, respectively.

Among the higher frequency bands, the 1681- cm^{-1} band for K^+ is assumed to be upshifted to 1692 cm^{-1} for Rb^+ and 1690 cm^{-1} for Cs^+ , which probably reflects a slight difference in coordination modes for Rb^+ and Cs^+ . The 1659- cm^{-1} band for K^+ almost doesn't change in frequency, compared with those for Rb^+ (1659 cm^{-1}) and Cs^+ (1657 cm^{-1}). However, the 1659- cm^{-1} band for K^+ dramatically reduces in intensity upon coordinating Na^+ or Li^+ , whereas the band intensity reduced moderately for Cs^+ (Fig. 4b). The 1659- cm^{-1} band is close to the typical frequency for an α -helix (1654 cm^{-1}). This frequency was insensitive to the type of alkali metal cation. To gain further insight, we analyzed the amide-II vibration.

Table 1 Vibrational frequencies of KcsA in the presence of each monovalent cation at 1700–1600 cm^{-1} (amide-I vibration)

cation		peak frequency (cm^{-1})			
Li ⁺		1659	1650	1639	1627
Na ⁺			1650	1639	1627
K ⁺	1681	1669	1659		
Rb ⁺	1692	1669	1659		
Cs ⁺	1690		1657		

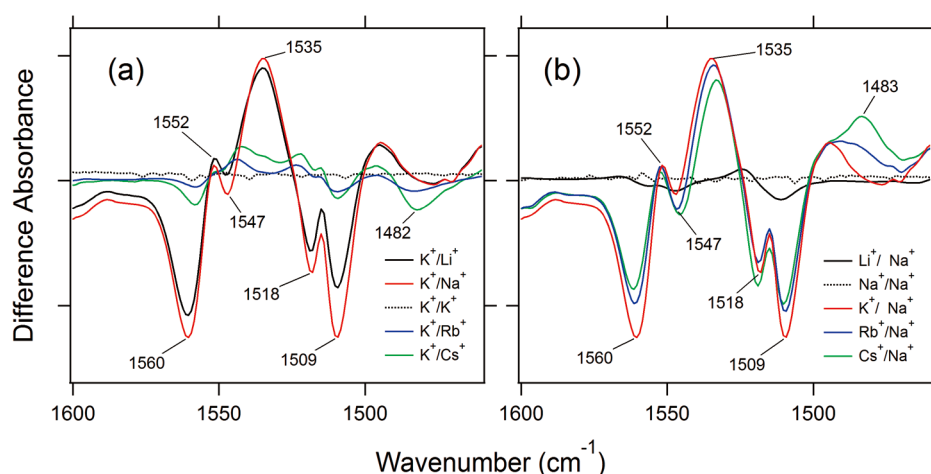


Figure 5 ATR-FTIR difference spectra of KcsA in the amide-II region (1600–1460 cm^{-1}), reproduced from Figure 2. (a) The K^+ -minus- Li^+ (black solid curve), K^+ -minus- Na^+ (red curve), K^+ -minus- K^+ (black dotted curve), K^+ -minus- Rb^+ (blue curve), and K^+ -minus- Cs^+ (green curve) spectra. (b) The Li^+ -minus- Na^+ (black solid curve), Na^+ -minus- Na^+ (black dotted curve), K^+ -minus- Na^+ (red curve), Rb^+ -minus- Na^+ (blue curve), and Cs^+ -minus- Na^+ (green curve) spectra. One division of the y-axis represents 0.005 absorbance units.

Amide-II Vibrations of KcsA Interacting with Alkali Metal Cations. Figure 5a and 5b compare FTIR difference spectra between K^+ and the other cations, and between Na^+ and the other cations, respectively, in the amide-II vibrational region. The cation dependence of the intensity of the amide-II bands is basically similar to that of amide-I bands, such that the spectral changes are categorized into two patterns: one for KcsA(K^+), KcsA(Rb^+) and KcsA(Cs^+) and another for KcsA(Na^+) and KcsA(Li^+). Table 2 shows the characteristic amide-II frequencies of KcsA with each cation. KcsA(K^+), KcsA(Rb^+), and KcsA(Cs^+) possess a strong peak at 1535 cm^{-1} , whereas KcsA(Na^+) and KcsA(Li^+) possess two strong peaks at 1560 and 1509 cm^{-1} . Negligible spectral changes in the amide-II region upon exchanging Na^+ with Li^+ suggest structural similarity between KcsA(Na^+) and KcsA(Li^+) (Fig. 5b). The amide-II bands at 1535 and 1560 cm^{-1} are relatively close to the typical amide II frequency of an α -helical protein (1550–1540 cm^{-1}), while 1509 cm^{-1} is a much lower frequency. The bands at 1535 and 1560 cm^{-1} may be explained by a change in hydrogen bonding of the amide N-H groups of the main chain upon replacement of the cations. In contrast, the band at 1509 cm^{-1} for KcsA(Na^+) and KcsA(Li^+) may represent a very weak hydrogen bond of an amide N-H group of the peptide backbone. Another notable negative

band was observed at 1518 cm^{-1} in the difference spectra that included KcsA(Na^+) and KcsA(Li^+). We already assigned the 1518- cm^{-1} band in KcsA(Na^+) to a phenol ring vibration of Tyr78 by using the Y78F mutant protein [36]. Therefore, this result strongly suggests that the structures of the filter around Tyr78 in the Na^+ and Li^+ conditions resemble each other.

In the spectral region below 1500 cm^{-1} , we observed a systematic increase of negative (Fig. 5a) and positive (Fig. 5b) bands around 1483 cm^{-1} , in accordance with the increase of the ionic radius of the alkali metal cations (K^+ , Rb^+ , and Cs^+). We have not identified the origin of the bands, but they may be attributed to some vibrational mode of a side chain. One possible candidate is a $\nu(\text{CC})$ and/or $\delta(\text{CH})$ mode of residues Trp67 and Trp68, which are on the pore helix. These spectral changes might be correlated with structural changes of KcsA that occur upon accommodating the larger alkali metal cations.

The spectral analysis of the amide-I and -II vibrations clearly distinguished those measured in K^+ , Rb^+ and Cs^+ solutions from those in Na^+ and Li^+ solutions. These distinct spectral patterns for these ion species strongly suggest that amide-I and -II signals mainly monitor the vibrations of the peptide backbone near or on the selectivity filter. However, contributions from the peptide backbone outside the selectivity filter were suggested. Similar to the amide-I band at 1659- cm^{-1} , the small amide-II signals at 1547 cm^{-1} are typical bands originating from an α -helix (1550–1540 cm^{-1}). The 1547- cm^{-1} bands for Na^+ and Li^+ show slight changes in their frequencies upon replacement with the other alkali metal cations (1552 cm^{-1} for K^+ , Rb^+ , and Cs^+). Thus, it is likely that the cation-type insensitive amide I band at 1654 cm^{-1} and the amide II band at 1547 or 1552 cm^{-1} originate from the same helix in KcsA, whose most probable candidate is a pore helix near the selectivity filter.

Table 2 Vibrational frequencies of KcsA in the presence of each monovalent cation at 1600–1450 cm^{-1} (amide-II vibration)

cation	peak frequency (cm^{-1})		
Li^+	1560	1547	1509
Na^+	1560	1547	1509
K^+	1552		1535
Rb^+	1552		1535
Cs^+	1552		1535

The nearly identical spectral frequencies of the amide-I and -II signals for Na⁺ and Li⁺, including the 1518-cm⁻¹ band for Tyr78, strongly suggest that the selectivity filter adopts a collapsed conformation with Li⁺. There are some differences in the experimental conditions between those in the crystallography and our FTIR measurements. Among them, Li⁺ concentration was higher (150 mM) in the crystallography, and it cannot be ruled out that the collapsed conformation detected in our experiment at 50 mM Li⁺ may turn to the open conformation at higher Li⁺ concentration.

Comparisons to the simulation studies. The X-ray structures of KcsA enabled computational studies that gave insights into the interactions of various cations with KcsA [42,43]. Recently, a theoretical approach based on MD simulation and spectral modeling was applied to KcsA. This analysis accurately reproduced the experimental difference spectrum of KcsA upon replacing K⁺ with Na⁺ [44]. It showed that the amide-I band at approximately 1680 cm⁻¹ originates from the carbonyl groups in the selectivity filter, while the band at approximately 1660 cm⁻¹ originates from the pore helices connected with the filter. These arguments are consistent with our results. Moreover, it was proposed that the band at approximately 1630 cm⁻¹ is representative of a vibrational mode involving four carbonyl groups interacting with Na⁺ (B-site mode). In our data, the bands at around 1680 cm⁻¹ were shifted among the ions but those at approximately 1660 cm⁻¹ were not: K⁺ (1681 cm⁻¹, 1659 cm⁻¹), Rb⁺ (1692 cm⁻¹, 1659 cm⁻¹), and Cs⁺ (1690 cm⁻¹, 1657 cm⁻¹). These observations suggest that the bands at around 1680 cm⁻¹ reflect direct interactions between the ions and the C=O groups in the filter, and that the bands at approximately 1660 cm⁻¹ include structural information from other parts of KcsA (probably the pore helix, as proposed by Stevenson *et al.*). The 1627-cm⁻¹ band of KcsA(Na⁺) is assumed to be same as the B-site mode in the literature; this band exhibits no frequency change in KcsA(Li⁺) at all. The mode might be insensitive to the difference in the ion radii of Na⁺ and Li⁺. It has been reported that the amide I vibrations of a hydrated α helix appear at a lower frequency than those of a typical α helix [45–47]. Therefore, the low-frequency vibrations of the amide-I mode (1639, and 1627 cm⁻¹) may be explained not only by a four-coordinate structure with Na⁺, but also by water hydration. A similar argument may be applicable to KcsA(Li⁺).

Conclusion

Ion-exchange-induced ATR-FTIR difference spectroscopy has provided valuable information about ion–protein interactions in the KcsA potassium channel. From the patterns of the spectral changes in the amide-I and -II regions for the various ion species, the origin of these bands has been examined. In this potassium channel, ions are solvated by the backbone carbonyls of the selectivity filter, and these interactions further affect the pore helix through hydrogen bonds.

These intimate interactions between ions and the channel lead to various spectral changes. More specifically, we have identified a cation-type sensitive amide-I band at 1681 cm⁻¹ and a cation-type insensitive amide-I band at 1659 cm⁻¹ in the difference spectra of KcsA. The former band reflects the differences in coordination structure of the C=O groups in the selectivity filter with the alkali metal cations. The latter band may be caused by the structural change of an α helix outside the selectivity filter. The similar spectral changes for Na⁺ and Li⁺ suggest that the filter structure in the case of Li⁺ would be in a collapsed conformation similar to that seen in the case of Na⁺.

Acknowledgements

This work was supported by grants from Japanese Ministry of Education, Culture, Sports, Science, and Technology to Y. F. (20050013, 21023014, 21026016, 22770159, 22247024, 26708002), H. S. (24249013), S. O. (26253014) and H. K. (20108014, 22247024).

We thank Prof. Masayo Iwaki and Drs. Masayuki Iwamoto and Takashi Sumikama for their valuable discussions. The authors would like to thank Enago (www.enago.jp) for the English language review.

Conflicts of Interest

All authors declare that they have no conflict of interest.

Author Contributions

Y. F., S. O., and H. K. directed the project. Y. F., H. S., S. O., and H. K. co-wrote the manuscript. H. S. and Y. A. prepared KcsA samples. Y. F. and Y. A. performed ATR-FTIR analysis.

References

- [1] Schrepf, H., Schmidt, O., Kummerlen, R., Hinnah, S., Müller, D., Betzler, M., *et al.* A prokaryotic potassium ion channel with two predicted transmembrane segments from *Streptomyces lividans*. *EMBO J.* **14**, 5170–5178 (1995).
- [2] Doyle, D. A., Morais Cabral, J., Pfuetzner, R. A., Kuo, A., Gulbis, J. M., Cohen, S. L., *et al.* The structure of the potassium channel: molecular basis of K⁺ conduction and selectivity. *Science* **280**, 69–77 (1998).
- [3] Ando, H., Kuno, M., Shimizu, H., Muramatsu, I. & Oiki, S. Coupled K⁺-water flux through the HERG potassium channel measured by an osmotic pulse method. *J. Gen. Physiol.* **126**, 529–538 (2005).
- [4] Oiki, S., Iwamoto, M. & Sumikama, T. A mesoscopic approach to understanding the mechanisms underlying the ion permeation on the discrete-state diagram. *J. Gen. Physiol.* **136**, 363–365 (2010).
- [5] Iwamoto, M. & Oiki, S. Counting ion and water molecules in a streaming file through the open-filter structure of the K channel. *J. Neurosci.* **31**, 12180–12188 (2011).
- [6] Oiki, S., Iwamoto, M. & Sumikama, T. Cycle flux algebra for

- ion and water flux through the KcsA channel single-file pore links microscopic trajectories and macroscopic observables. *PLoS One* **6**, e16578 (2011).
- [7] Phongphanphane, S., Yoshida, N., Oiki, S. & Hirata, F. Probing “ambivalent” snug-fit sites in the KcsA potassium channel using three-dimensional reference interaction site model (3D-RISM) theory. *Pure and Applied Chemistry* **86**, 97–104 (2014).
- [8] Oiki, S. Channel function reconstitution and re-animation: a single-channel strategy in the postcrystal age. *J. Physiol.* **593**, 2553–2573 (2015).
- [9] Splitt, H., Meuser, D., Borovok, I., Betzler, M. & Schrempf, H. Pore mutations affecting tetrameric assembly and functioning of the potassium channel KcsA from *Streptomyces lividans*. *FEBS Lett.* **472**, 83–87 (2000).
- [10] Zhou, Y., Morais-Cabral, J. H., Kaufman, A. & MacKinnon, R. Chemistry of ion coordination and hydration revealed by a K⁺ channel-Fab complex at 2.0 Å resolution. *Nature* **414**, 43–48 (2001).
- [11] Zhou, Y. & MacKinnon, R. The occupancy of ions in the K⁺ selectivity filter: charge balance and coupling of ion binding to a protein conformational change underlie high conduction rates. *J. Mol. Biol.* **333**, 965–975 (2003).
- [12] Lockless, S. W., Zhou, M. & MacKinnon, R. Structural and thermodynamic properties of selective ion binding in a K⁺ channel. *PLoS Biol.* **5**, e121 (2007).
- [13] Thompson, A. N., Kim, I., Panosian, T. D., Iverson, T. M., Allen, T. W. & Nimigeon, C. M. Mechanism of potassium-channel selectivity revealed by Na⁺ and Li⁺ binding sites within the KcsA pore. *Nat. Struct. Mol. Biol.* **16**, 1317–1324 (2009).
- [14] Gerwert, K. Molecular reaction mechanisms of proteins monitored by time-resolved FTIR-spectroscopy. *Biol. Chem.* **380**, 931–935 (1999).
- [15] Kandori, H., Sudo, Y. & Furutani, Y. Protein-protein interaction changes in an archaeal light-signal transduction. *J. Biomed. Biotechnol.* **2010**, 424760 (2010).
- [16] Noguchi, T. Light-induced FTIR difference spectroscopy as a powerful tool toward understanding the molecular mechanism of photosynthetic oxygen evolution. *Photosynth. Res.* **91**, 59–69 (2007).
- [17] Radu, I., Schleegeer, M., Bolwien, C. & Heberle, J. Time-resolved methods in biophysics. 10. Time-resolved FT-IR difference spectroscopy and the application to membrane proteins. *Photochem. Photobiol. Sci.* **8**, 1517–1528 (2009).
- [18] Furutani, Y., Shibata, M. & Kandori, H. Strongly hydrogen-bonded water molecules in the Schiff base region of rhodopsins. *Photochem. Photobiol. Sci.* **4**, 661–666 (2005).
- [19] Kandori, H. Role of internal water molecules in bacteriorhodopsin. *Biochim. Biophys. Acta* **1460**, 177–191 (2000).
- [20] Noguchi, T. FTIR detection of water reactions in the oxygen-evolving centre of photosystem II. *Philos. Trans. R Soc. Lond. B Biol. Sci.* **363**, 1189–1194; discussion 1194–1185 (2008).
- [21] Furutani, Y., Fujiwara, K., Kimura, T., Kikukawa, T., Demura, M. & Kandori, H. Dynamics of Dangling Bonds of Water Molecules in *pharaonis* Halorhodopsin during Chloride Ion Transportation. *J. Phys. Chem. Lett.* **3**, 2964–2969 (2012).
- [22] Ataka, K. & Heberle, J. Biochemical applications of surface-enhanced infrared absorption spectroscopy. *Anal. Bioanal. Chem.* **388**, 47–54 (2007).
- [23] Rich, P. R. & Iwaki, M. Methods to probe protein transitions with ATR infrared spectroscopy. *Mol. Biosyst.* **3**, 398–407 (2007).
- [24] Iwaki, M., Giotta, L., Akinsiku, A. O., Schägger, H., Fisher, N., Breton, J., *et al.* Redox-induced transitions in bovine cytochrome bc₁ complex studied by perfusion-induced ATR-FTIR spectroscopy. *Biochemistry* **42**, 11109–11119 (2003).
- [25] Ataka, K., Giess, F., Knoll, W., Naumann, R., Haber-Pohlmeier, S., Richter, B., *et al.* Oriented attachment and membrane reconstitution of His-tagged cytochrome *c* oxidase to a gold electrode: *in situ* monitoring by surface-enhanced infrared absorption spectroscopy. *J. Am. Chem. Soc.* **126**, 16199–16206 (2004).
- [26] Iwaki, M. & Rich, P. R. Direct detection of formate ligation in cytochrome *c* oxidase by ATR-FTIR spectroscopy. *J. Am. Chem. Soc.* **126**, 2386–2389 (2004).
- [27] Iwaki, M. & Rich, P. R. An IR study of protonation changes associated with heme-heme electron transfer in bovine cytochrome *c* oxidase. *J. Am. Chem. Soc.* **129**, 2923–2929 (2007).
- [28] le Coutre, J., Turk, E., Kaback, H. R. & Wright, E. M. Ligand-induced differences in secondary structure of the *Vibrio parahaemolyticus* Na⁺/galactose cotransporter. *Biochemistry* **41**, 8082–8086 (2002).
- [29] Iwaki, M., Cotton, N. P. J., Quirk, P. G., Rich, P. R. & Jackson, J. B. Molecular recognition between protein and nicotinamide dinucleotide in intact, proton-translocating transhydrogenase studied by ATR-FTIR Spectroscopy. *J. Am. Chem. Soc.* **128**, 2621–2629 (2006).
- [30] Lórenz-Fonfria, V. A., Granell, M., León, X., Leblanc, G. & Padrós, E. In-plane and out-of-plane infrared difference spectroscopy unravels tilting of helices and structural changes in a membrane protein upon substrate binding. *J. Am. Chem. Soc.* **131**, 15094–15095 (2009).
- [31] Guijarro, J., Engelhard, M. & Siebert, F. Anion uptake in halorhodopsin from *Natromonas pharaonis* studied by FTIR spectroscopy: consequences for the anion transport mechanism. *Biochemistry* **45**, 11578–11588 (2006).
- [32] Kitade, Y., Furutani, Y., Kamo, N. & Kandori, H. Proton release group of *pharaonis* phoborhodopsin revealed by ATR-FTIR spectroscopy. *Biochemistry* **48**, 1595–1603 (2009).
- [33] Furutani, Y., Kimura, T. & Okamoto, K. Development of a rapid Buffer-exchange system for time-resolved ATR-FTIR spectroscopy with the step-scan mode. *BIOPHYSICS* **9**, 123–129 (2013).
- [34] Sudo, Y., Kitade, Y., Furutani, Y., Kojima, M., Kojima, S., Homma, M., *et al.* Interaction between Na⁺ ion and carboxylates of the PomA-PomB stator unit studied by ATR-FTIR spectroscopy. *Biochemistry* **48**, 11699–11705 (2009).
- [35] Furutani, Y., Murata, T. & Kandori, H. Sodium or lithium ion-binding-induced structural changes in the K-ring of V-ATPase from *Enterococcus hirae* revealed by ATR-FTIR spectroscopy. *J. Am. Chem. Soc.* **133**, 2860–2863 (2011).
- [36] Furutani, Y., Shimizu, H., Asai, Y., Fukuda, T., Oiki, S. & Kandori, H. ATR-FTIR Spectroscopy Revealing the Different Vibrational Modes of the Selectivity Filter Interacting with K⁺ and Na⁺ in the Open and Collapsed Conformations of the KcsA Potassium Channel. *J. Phys. Chem. Lett.* **3**, 3806–3810 (2012).
- [37] Jiang, X., Zaitseva, E., Schmidt, M., Siebert, F., Engelhard, M., Schlesinger, R., *et al.* Resolving voltage-dependent structural changes of a membrane photoreceptor by surface-enhanced IR difference spectroscopy. *Proc. Natl. Acad. Sci. USA* **105**, 12113–12117 (2008).
- [38] Yamakata, A., Shimizu, H., Osawa, M. & Oiki, S. Structural changes of the KcsA potassium channel upon application of the electrode potential studied by surface-enhanced IR absorption spectroscopy. *Chem. Phys.* **419**, 224–228 (2013).
- [39] Yamakata, A., Shimizu, H. & Oiki, S. Surface-enhanced IR absorption spectroscopy of the KcsA potassium channel upon application of an electric field. *Phys. Chem. Chem. Phys.*, **17**, 21104–21111 (2015).
- [40] Iwamoto, M., Shimizu, H., Inoue, F., Konno, T., Sasaki, Y. C.

- & Oiki, S. Surface structure and its dynamic rearrangements of the KcsA potassium channel upon gating and tetrabutylammonium blocking. *J. Biol. Chem.* **281**, 28379–28386 (2006).
- [41] Barth, A. & Zscherp, C. What vibrations tell us about proteins. *Q. Rev. Biophys.* **35**, 369–430 (2002).
- [42] Egwolf, B. & Roux, B. Ion selectivity of the KcsA channel: a perspective from multi-ion free energy landscapes. *J. Mol. Biol.* **401**, 831–842 (2010).
- [43] Phongphanphanee, S., Yoshida, N., Oiki, S. & Hirata, F. Distinct configurations of cations and water in the selectivity filter of the KcsA potassium channel probed by 3D-RISM theory. *J. Mol. Liq.* **200**, 52–58 (2014).
- [44] Stevenson, P., Gotz, C., Baiz, C. R., Akerboom, J., Tokmakoff, A. & Vaziri, A. Visualizing KcsA Conformational Changes upon Ion Binding by Infrared Spectroscopy and Atomistic Modeling. *J. Phys. Chem. B* **119**, 5824–5831 (2015).
- [45] Kimura, T., Maeda, A., Nishiguchi, S., Ishimori, K., Morishima, I., Konno, T., *et al.* Dehydration of main-chain amides in the final folding step of single-chain monellin revealed by time-resolved infrared spectroscopy. *Proc. Natl. Acad. Sci. USA* **105**, 13391–13396 (2008).
- [46] Manas, E. S., Getahun, Z., Wright, W. W., DeGrado, W. F. & Vanderkooi, J. M. Infrared spectra of amide groups in α -helical proteins: Evidence for hydrogen bonding between helices and water. *J. Am. Chem. Soc.* **122**, 9883–9890 (2000).
- [47] Walsh, S. T. R., Cheng, R. P., Wright, W. W., Alonso, D. O. V., Daggett, V., Vanderkooi, J. M., *et al.* The hydration of amides in helices; a comprehensive picture from molecular dynamics, IR, and NMR. *Protein Sci.* **12**, 520–531 (2003).